DOI: 10.15825/1995-1191-2022-2-71-82

TESTING OF THE pHEMA HYDROGEL AS AN IMPLANTATION MATERIAL FOR REPLACEMENT OF OSTEOCHONDRAL DEFECTS IN ANIMALS

E.B. Makarova[1, 2], M.A. Korch[3], F.A. Fadeyev[1, 4], D.G. Bliznets[2], A.V. Bugayova[1, 5], T.F. Shklyar[1, 5], A.P. Safronov[5], K.A. Nokhrin[5], F.A. Blyakhman[1, 5]

[1] Ural State Medical University, Ekaterinburg, Russian Federation
[2] Chaklin Ural Institute of Traumatology and Orthopedics, Ekaterinburg, Russian Federation
[3] Ural State Agrarian University, Ekaterinburg, Russian Federation
[4] Institute of Medical Cell Technology, Ekaterinburg, Russian Federation
[5] Ural Federal University, Ekaterinburg, Russian Federation

Objective: to evaluate the features of reparative chondrogenesis and osteogenesis in animal experiments with the implantation of porous poly(2-hydroxyethyl methacrylate) (pHEMA) hydrogel into osteochondral defects. **Materials and methods.** Cylindrical pHEMA implants (5 mm in diameter) were synthesized by radical polymerization. The implants were subjected to light microscopy and mechanical tests to characterize the structure and viscoelastic properties of the material. In experimental group #1, four pHEMA specimens were implanted into formed defects in the distal femoral epiphysis of rabbits. In experimental group #2, allogeneic chondrocytes were applied to the surface of four specimens before implantation. In the control series, four defects were not replaced with implants. Tissue regeneration was investigated by morphological and morphometric methods 30 days after operation. **Results.** The pHEMA implants were heterogeneous specimens with irregularly shaped pores – up to 30 × 10 μm at the surface and 300 × 120 μm inside. With >10% static compressive stress, the Young's modulus was 54.7 kPa. For dynamic stress, increased frequency of compression-relaxation cycles from 0.01 Hz to 20.0 Hz led to increased storage modulus from 20 kPa to 38 kPa on average, and increased loss modulus from 2 kPa to 10 kPa. Indicators of semi-quantitative assessment of local inflammatory response to pHEMA implantation had the following values in points: pHEMA, 4.7 ± 0.3; pHEMA with allogeneic chondrocytes, 6.0 ± 1.0; control, 4.3 ± 0.3. The ratio of connective, bone, and cartilage tissues proper in the regenerates had the following respective values: pHEMA, 79%, 20%, 1%; pHEMA with chondrocytes, 82%, 16%, 2%; control, 9%, 74%, 17%. **Conclusion.** In a short-term experiment, pHEMA implants did not trigger a pronounced inflammatory response in the surrounding tissues and can be classified as biocompatible materials. However, the tested implants had low conductivity with respect to bone and cartilage cells, which can be improved by stabilizing the pore size and increasing the rigidity when synthesizing the material.

Keywords: osteochondral defects, implants, pHEMA hydrogel, physical properties, biocompatibility, cartilage tissue, bone tissue.

INTRODUCTION

Focal osteochondral lesions are commonly found in 61–63% of patients during arthroscopy [1]. The spontaneous repair ability of the articular cartilage tissue is very limited, and their presence provokes deforming osteoarthritis and reduces patients' quality of life [1]. On this basis, treatment of osteochondral injuries of the joint is an urgent task today.

To stimulate the regeneration of articular cartilage, a number of techniques, which have shown satisfactory medium-term treatment outcomes, are used. They include mosaicplasty [2], autochondrogenesis (AMIC) induced on a cell culture scaffold [3], autologous chondrocyte transplantation (ACI) [4], including those associated with collagen matrix (MACT/MACI) [5], and introduction of mesenchymal stromal cells [6]. At the same time, there is yet no method of treatment that provides organ-specific restoration of hyaline cartilage and complete long-term clinical remission [7]. This fact forces us to look for new ways to replace cartilage defects, including new cell transplantation matrices.

A wide range of materials for cellular matrices is known, among which hydrogels occupy a significant niche. A gel is a polymer swollen in a solvent; its composition can contain up to 99% liquid. Synthetic hydrogels are considered to be biomimetics of biological tissues, since with an appropriate chemical composition

Corresponding author: Felix Blyakhman. Address: 3, Repin str., Ekaterinburg, 620028, Russian Federation. Phone: (343) 214-86-96. E-mail: feliks.blyakhman@urfu.ru

and certain physical and/or chemical influences, they demonstrate similar mechanical properties to living tissues [8, 9].

In this study, the pHEMA hydrogel was used as the material for osteochondral implants. It is known that pHEMA is nontoxic, inert, and biocompatible [10]. Through controlled synthesis, the physical properties of pHEMA can be approximated to those of biological tissues. In particular, the viscoelastic properties of pHEMA, its oxygen permeability, and its solvent content can match the characteristics of the extracellular matrix [11].

The biocompatibility of pHEMA and its physicochemical properties has made it useful in the manufacture of contact lenses, artificial corneas, drug delivery systems, and matrices for controlled stem cell differentiation [12]. In orthopedics, the possibility of using pHEMA for fabrication of artificial cartilage, nucleus pulposus of the intervertebral disc prosthesis, and its use as a mechanical vibration damper in the fabrication of a total intervertebral disc endoprosthesis is discussed [11, 13].

In terms of application of synthetic materials in medicine, pHEMA hydrogels have an advantage associated with the possibility of creating various morphological structures in the form of pores during synthesis [14]. The porous structure of pHEMA makes it possible to introduce various bioactive compounds, including those with antimicrobial activity [15]. Besides, porous synthetic hydrogels have proven themselves as three-dimensional cell culture matrices used in replacement therapy and regenerative medicine [12].

Based on the above, the aim of this study was to investigate cartilage and bone tissue regeneration during the filling of osteochondral defects in the femoral epiphysis with pHEMA porous hydrogel implants in in vivo animal experiments. The results of assessment of the structure and viscoelastic properties of the pHEMA implants, as well as data on the course of tissue reparative processes after implantation of hydrogels without cells and with allogeneic chondrocytes are presented.

MATERIALS AND METHODS

Synthesis of pHEMA-based implants

Synthetic pHEMA hydrogels were obtained by radical polymerization in an aqueous solution of monomer (hydroxyethyl methacrylate, HEMA) at 70 °C in the presence of a crosslinking agent, N,N'-methylenediacrylamide (MDAA). The monomer concentration was 2 mol/dm^3 (2 M) and the MDAA concentration was 0.02 mol/dm^3 (0.02 M). This ensured the formation of a mesh polymer structure in which the molar ratio of the mesh nodes to the links in the linear fragments was 1 : 100. We used 3 mM ammonium persulfate as a polymerization initiator. Polymerization was carried out in cylindrical polyethylene molds for one hour, after which the samples were removed from the molds and washed in distilled water for two weeks with daily water changes.

As a result, pHEMA specimens, ~5 mm in diameter and 120–150 mm long, were obtained, after which they were shortened with a scalpel to the implant size (~5.5 mm). To validate the elastic properties of pHEMA, specimens with a larger diameter (~9 mm) were synthesized.

pHEMA mechanical testing

The viscoelastic properties of the gels were evaluated on special mechanical testing equipment, and is described in detail in our earlier publications [16, 17]. Briefly, the mechanical testing setup contained precision force and displacement transducers, and a linear electromagnetic motor to give the specimens arbitrarily shaped deformations. Cylindrical pHEMA specimens, ~9 mm in diameter and ~5 mm in height, were placed into a cuvette filled with a solution in which the gel was pre-swollen. One end of the sample was rigidly attached to the force transducer and the other end to the motor lever.

To obtain the stress-strain relation, the specimens were given stepwise compressive strains with a 50 μm step and the value of the elastic force arising in the specimen was recorded. To determine the rheological characteristics of the material, the storage modulus (G') and loss modulus (G''), sinusoidal compressive strains with an amplitude of ~3% of the initial height of the specimen and frequency 0.01 to 20 Hz were applied to the specimens. The method of setting and analyzing the effects of low-amplitude periodic deformations is widely used to determine the viscoelastic properties of materials, including pHEMA [18].

Experimental animals and study groups

Sexually mature Soviet Chinchilla male rabbits (age 5 months, weight 2.8–3.5 kg), with animal certificate No. 2020/2KSh dated April 12, 2020, were used in the work. Management, surgical interventions, and euthanasia were performed in accordance with the requirements and principles of biomedical research involving vertebrate animals set forth in the European Convention (1986) and its protocol of 1998. The experimental protocol was approved by the Ethical Committee of the Ural State Medical University (protocol No. 2 of February 28, 2020).

In 6 rabbits, standard large osteochondral defects were created in the articular patellar surface of the metaphysis of both femurs (n = 12). Such defects did not result in complete tissue replacement during the spontaneous reparative process, which corresponds to the literature [19]. Throughout the experiment, no animal death or purulent complications were observed. The animals were agile, their support ability and the correct position

of the limbs were preserved. One rabbit was used as a chondrocyte donor.

The animals were divided into 3 groups of 2 rabbits each. In the control group (CG), the defects were not replaced with implants (n = 4). In the experimental group #1 (EG-1), the defects were replaced with pHEMA implants (n = 4); in experimental group #2 (EG-2), the defects were filled with pHEMA implants with allogeneic chondrocytes adhered to them (n = 4). Thirty days after surgery, all animals were removed from the experiment, after which the femur metaphysis were examined.

Preparation of pHEMA implants with adherent chondrocytes

Chondrocyte culture was obtained from the cartilage tissue of the rabbit knee joint used as a donor. Chondrocytes were isolated from the tissue by dissociation with collagenase-I. For this purpose, the cartilage tissue of the articular surfaces of the hip and knee joints was crushed and incubated at 37 °C in 0.3 mg/ml collagenase solution for 90 minutes. The solution was then replaced with a fresh one in 0.5 mg/ml collagenase concentration; incubation was performed for 16 hours at 37 °C with this solution.

Dissociated cells were grown as a monolayer culture in culture vials using specialized chondrocyte growth medium kit (Cell Applications, Inc.) in a CO_2 incubator (37 °C, 5% CO_2, 100% relative humidity). Once the monolayer reached 70% confluence, the cells were transplanted to a second passage. Cells were removed from the plastic using a 0.25% trypsin solution with EDTA. Chondrocytes from the second passage were used for seeding on the implant. The cell phenotype was confirmed using Alcian blue stain and nuclear red stain.

Chondrocytes were seeded on one of the flat surfaces of high-density pHEMA implants (300,000 cells/cm^2 implant surface). For this purpose, sterile hydrogels were placed vertically in a Petri dish, close to each other, and filled with a chondrocytic medium above the level of their upper edge. Chondrocytes were removed from the plastic with trypsin and resuspended in the chondrocytic medium. The obtained suspension was applied to the implant-coating medium, after which the cells were deposited on the implant surface. The implants were incubated for one day in a CO_2 incubator, and then used for implantation in rabbits.

To confirm chondrocyte adhesion on the implant surface, some samples were fixed and stained with pyrazolone yellow (cytoplasm) and DAPI (nuclei) according to the technique described earlier [17]. Fluorescence microscopy of the stained samples confirmed the adhesion of chondrocytes on the hydrogel surface. At the same time, the attached cells were irregularly distributed on the gel surface, with the formation of dense multilayer clusters.

Surgical procedure for pHEMA implantation

Surgical interventions were performed under general anesthesia (intramuscularly – Rometar 2% – 8 mg/kg (Rometar 2% Spofa, Prague, Czech Republic), isoletil – 6 mg/kg (Zoletil-100, VirbacSanteAnimale). Medial access with dissection of the patellar-retaining ligament was used to perform arthrotomy with surgical dislocation of the patella laterally. A cylindrical osteochondral defect (Fig. 1, a) was formed on the anterior surface of the distal femoral epiphysis in the area of the patellofemoral junction surface with a 5.0-mm diameter drill with a stopper.

Two transverse canals were formed in the distal femoral epiphysis with a 1.5-mm diameter wire through the lateral cortical bone walls at the defect level and 4 mm proximal to the defect. Implants, 5 mm in diameter and 5.5 mm in height, were inserted into the defects (Fig. 1, b) and fixed to the defect walls with transverse sutures through the transverse canals (Fig. 1, c, d). The surgical wound was sutured in layers to restore the integrity of the ligament holding the patella.

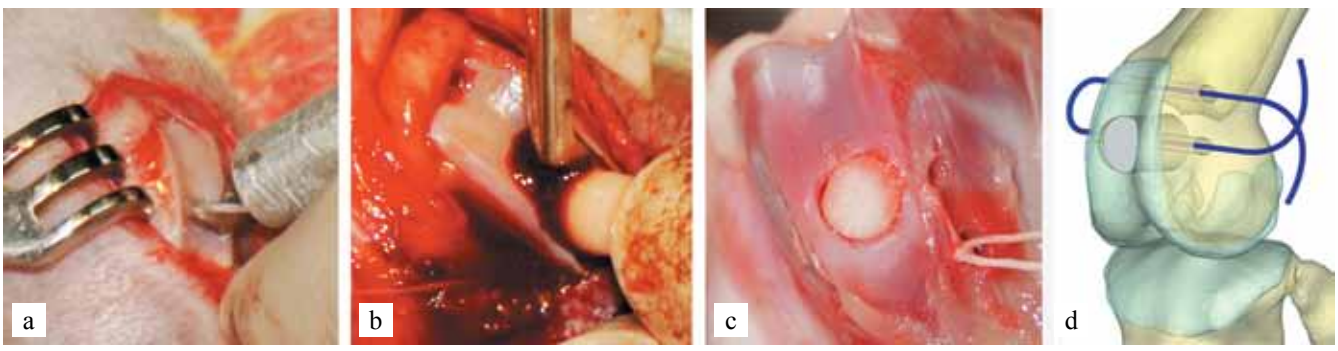

Fig. 1. Stages of implant insertion in a rabbit's femoral epiphysis. a, formation of a standard defect with a drill with a stopper; b, implant insertion; c, the view of the articular surface after implant placement; d, diagram showing implant localization and its fixation with transosseous sutures

Methodology of the morphological study

The material (distal femoral epiphysis) for morphological study was obtained immediately after the animals had been removed from the experiment. Femoral fragments were fixed in 10% neutral buffered formalin (BioOptica). Bone tissue was decalcified, and part of the bone material was embedded in paraffin. Under standard paraffin wiring protocol, the pHEMA material lost up to 1/2 of its volume, which deformed the delicate newly formed tissue surrounding the implants and disrupted the topographic unity of the preparation. Therefore, a part of bone fragments was poured into gelatin and subjected to cryotomy. Epimetaphyseal slices were made in the sagittal plane.

Hematoxylin and eosin were used as visual stains. Van Gieson's stain was used to identify the connective tissue components. Micros MS300 light microscope was used for descriptive morphology. Digitization of preparations and morphometric studies were performed on 3DHISTECH PANNORAMIC Midi scanning microscope using Pannoramic Viewer software.

Morphometric assessment of the regenerate included determination of the height of the supra-implantation regenerate, thickness of the peri-implantation capsule, depth of regenerating tissue sprouting into the implant pores, area and ratio of tissue components in the peri-implantation area, counting of chondrocytes and their isogenic groups in the newly formed cartilage tissue.

The local biological effect of the implants was determined by a semi-quantitative assessment of the inflammatory reaction [20]. Inflammatory response was characterized by the presence of necrosis zones, the number of pro-inflammatory cells – polymorphonuclear leukocytes, mast cells, lymphocytes, macrophages, plasma cells and giant multinucleated cells in the field of view under ×400 magnification.

Statistical analysis

The results are presented as $X \pm m$, where X is the arithmetic mean and m is the error of the arithmetic mean. The nonparametric Mann–Whitney U Test was used to assess differences between two independent samples. The acceptable level of statistical significance was $p \leq 0.05$. Statistical analysis of the data was performed using licensed software Statistica 6.0.

RESULTS

Features of the architecture of pHEMA implants

Synthetic pHEMA hydrogels have a number of structural features that distinguish them from other gels used for biomedical purposes, in particular, from the widespread polyacrylamide hydrogels. Unlike the latter, pHEMA hydrogels are a heterogeneous macroporous system [18]. The HEMA monomer is well soluble in water, while the pHEMA polymer has limited water solubility. Therefore, during hydrogel synthesis, the initially homogeneous monomer solution undergoes phase separation as polymerization proceeds. At the same time, the formed irregular polymer mesh separates from the aqueous medium and forms a macroporous structure, which is schematically shown in Fig. 2, a.

The structure of pHEMA contains large, irregularly shaped pores filled with liquid. The pore walls are formed by the irregular grid structure of pHEMA, which, in turn, also contains water and is permeable to dissolved salts and simple compounds (sugars, amino acids, etc.). The heterogeneous nature of pHEMA is manifested, in particular, by the fact that its samples are not transparent but are milky-white due to light scattering on the walls of macropores in the gel structure (Fig. 1, b, c).

Fig. 2 shows as an example the photos of cryosections of pHEMA implants recorded before and after the experiment (Fig. 2, b, c). It is clearly seen that in the depth

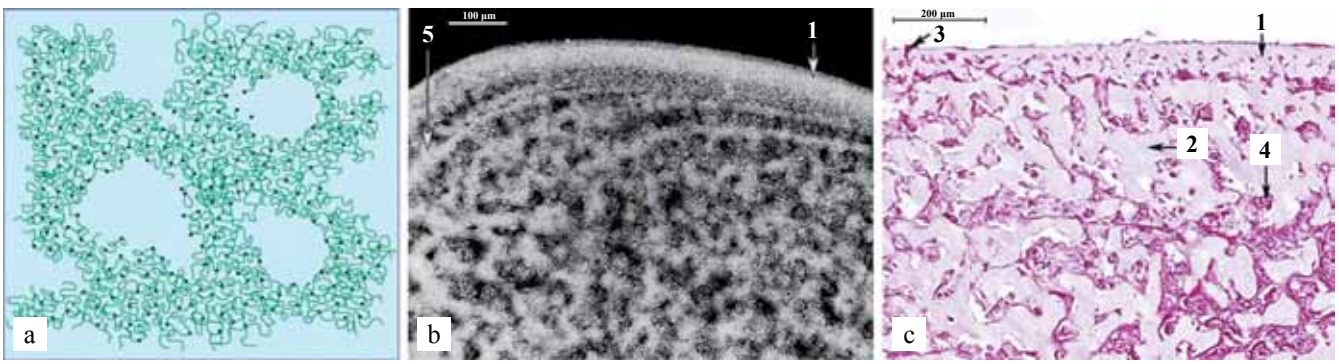

Fig. 2. a, diagram showing the molecular structure of synthetic pHEMA hydrogel. Lines are the linear fragments of polymer chains, dots represent mesh nodes; b, c, – implant imaging examples, light microscopy. b, pHEMA cryosection before experiment (100× magnification, color rendering inverted); c, pHEMA cryosection 30 days after implantation (200× magnification, H&E stain). 1, dense surface layer; 2, pHEMA; 3, pore communicating with the surface; 4, pores inside the implant with loose irregular connective tissue and osteoid; 5, concentric layers inside the implant containing small pores

of the samples, the pores (dark areas in Fig. 2, b, in Fig. 2, c the pores are filled with loose connective tissue) have an irregular shape, they do not exceed 300 μm in size on the long axis and 120 μm on the short axis. The surface dense layer of the implants, 20–150 microns wide, has much smaller pores (up to 30 μm on the long axis, up to 10 μm on the short axis), with a small number of pores communicating with the surface.

In general, the internal architecture of the implant can be characterized as a highly hydrated macroporous polymeric material with a high degree of structural heterogeneity.

Viscoelastic properties of pHEMA

Fig. 3 shows the results of mechanical tests of pHEMA samples in static (n = 5) and dynamic (n = 6) loading modes. The stress-strain dependences were obtained for the gel compression deformation with a 50 μm step (Fig. 3, a). It can be seen that mechanical stress in the gel increases with increasing strain. In general, the dependence is not linear, and qualitatively resembles the one for biological soft tissues [21]. On the curve, there are two areas in which the relationship is linear and is described by linear regression equation: the first – up to 5–6% deformation, the second – at deformations greater than 10%. The coefficient in the first term of the equation, defined as the slope of the tangent to the curve, corresponds to Young's modulus, whose value for the first and second parts of the curve is 19.6 kPa and 54.7 kPa, respectively.

Fig. 3, b illustrates the results of the mechanical test analysis of pHEMA in the dynamic load regime. The frequency-dependent values for the storage modulus (G') as a measure of gel elasticity and the loss modulus (G") as a characteristic of the object's viscosity are shown. It can be seen that at extremely low frequencies, pHEMA behaves more like an elastic body. The storage modulus is close to the Young's modulus determined in the static mode over the first range of small deformations. As the frequency of compression-relaxation cycles of gels increases from 0.01 Hz to 20.0 Hz, the storage modulus increases from 20 kPa to 38 kPa on average, and the loss modulus increases from 2 kPa to 10 kPa. That is, the contribution of the viscous component to the mechanical response of the gel to deformation begins to increase. In general, approximately the same dynamics of the moduli with a significant increase in the strain frequency indicates a good stabilization of the bonds in the structure of the pHEMA polymer network. This implies a high degree of gel wear resistance in the selected load range.

Macroscopic examination of osteochondral tissues

Thirty days after surgery in the CG, the articular surfaces of the distal femoral epiphysis showed irregularities and thickening in the areas near the defects (Fig. 4, a).

In EG-1 and EG-2, the spatial arrangement of the implants was maintained throughout the experiment. In EG-1, the implants were covered with thin regenerates with small gaping areas, and there were roller-like thickenings on the dorsal surface of the condyles (Fig. 4, b). The greatest changes in the articular surface were found in EG-2 – signs of regenerative hypertrophy in the form of valvular outgrowths throughout the dorsal surface of the distal epiphysis. The regenerates over the implants are thin with perforations (Fig. 4, c).

Microscopic examination of regenerates

The articular surfaces in the peri-implantation area had pronounced degenerative changes in the superficial and intermediate cartilage zones (Fig. 5), as well as signs of reactive-productive repair. In particular, animals of all series showed thickening on articular surfaces formed by bone trabeculae with signs of active osteogenesis, structured hyaline cartilage with fibrillated matrix, and broad perichondrium.

The structure of the articular surface regenerate differed in the animals of the experimental and control groups. In CG, the regenerate was formed by a broad

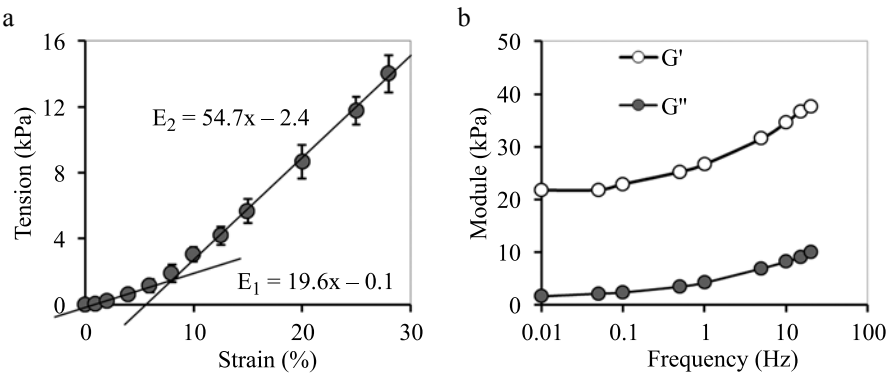

Fig. 3. Viscoelastic properties of pHEMA: a, relationship between mechanical stress in the gel and its deformation; b, storage modulus (G') and loss modulus (G'') versus angular frequency (representative graphs)

layer of partially structured hyaline-like cartilage with a thin layer of dense irregular connective tissue similar to perichondrium (Fig. 5, a). At the subchondral level and deeper, the cavity was filled with newly formed bone tissue; the subchondral plate was not restored. Repair processes were not completed.

In EG-1 and EG-2, the regenerates on the articular surface were formed by dense irregular connective tissue with loci of loose connective tissue and signs of active angiogenesis. Cartilage tissue regeneration occurred only at the edges of the implantation cavity; its main source of development was probably chondrocyte precursor cells from the subchondral bone tissue. In EG-1, the regenerate was formed by dense irregular connective tissue with high cellularity and relatively loosely arranged fibers (Fig. 5, b); in EG-2 (Fig. 5, c), it was represented by connective tissue with denser collagen fibers, which indicates its greater maturity. The area of the regenerate (the area corresponding to the cartilage projection before the defect was formed) in EG-1 and EG-2 was 2.9 and 2.3 times smaller than in CG ($p < 0.05$), respectively.

In EG-1 and EG-2, throughout the contact with the implantation bed, the implants were surrounded by connective-tissue capsules that included separate loci of chondrogenesis and osteogenesis. In EG-1 and EG-2, the capsules were formed by dense irregular connective tissue (Fig. 6, a, b). The capsule thickness in EG-1 and EG-2 (193 ± 77 μm and 180 ± 84 μm, respectively) and their areas did not differ significantly in the experimental group. In the peri-implant area between the newly formed bone trabeculae, pHEMA fragments were detected, indicating partial implant failure in vivo (Fig. 6, a).

The ratios of connective tissue proper (dense and loose), bone tissue, and cartilage tissue within the regenerates had the following respective values: pHEMA, 79%, 20%, 1%; pHEMA with chondrocytes, 82%, 16%, 2%; control, 9%, 74%, 17%. Cartilage tissue in EG-1 and EG-2 was represented by small non-vascular fields with single and small isogenic groups of chondrocytes (EG-2 showed a tendency to increase) with high cell density and little matrix volume, which indicated cartilage immaturity and distinguished the experimental groups from the control.

In both experimental groups, the loose connective tissue fibers "grew" into the open pores of the implant communicating with the surface. The entire depth of the pore spaces was predominantly filled with loose connective tissue with newly formed capillaries and small

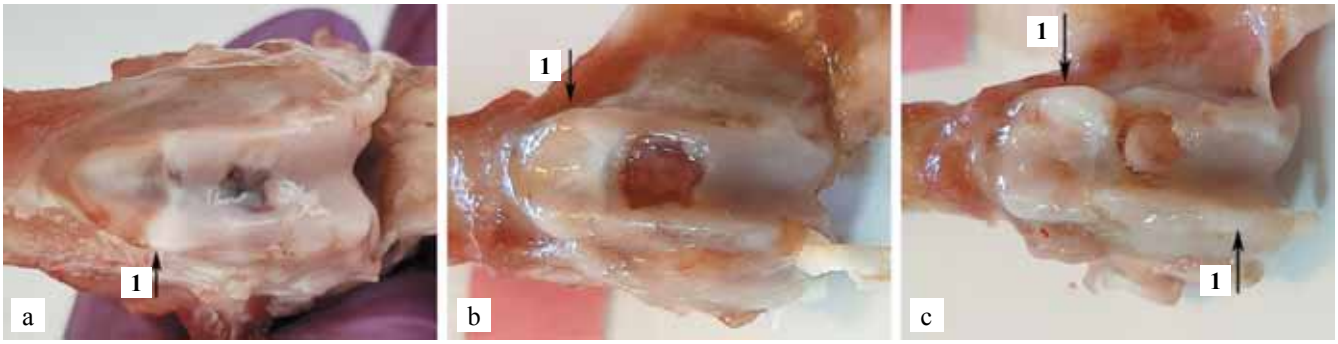

Fig. 4. Macro specimens of distal femoral epiphyses of rabbits, 30 days after surgery. a, defect not filled with implant; b, defect filled with pHEMA implant; c, defect filled with pHEMA implant with adherent allogeneic chondrocytes. 1, roller-shaped bone crest thickenings

Fig. 5. Regeneration of the articular surface (distal femoral epiphysis in rabbits) in the border area of the defect cavity, 30 days after surgery. H&E stain. Light microscopy, 100× magnification. a, control group; b, experimental group 1; c, experimental group 2. 1, articular cartilage; 2, cavity boundary; 3, newly formed reticulofibrous bone tissue; 4, newly formed cartilage tissue; 5, connective tissue proper on the implant surface; 6, implant

areas of bone tissue (Fig. 6, c, d). The pores of the lateral implant surfaces contacting the cavity bed contained foci of osteogenesis.

Microscopic assessment of local inflammatory response

A semi-quantitative evaluation of the local biological effects of the pHEMA implants revealed that the inflammatory response scores in the experimental groups were slightly higher than in the control (CG, 4.33 ± 0.33; EG-1, 4.7 ± 0.33; EG-2, 6.0 ± 1.0), but the differences were not statistically reliable. The inflammatory response scores were elevated mainly due to increased number of macrophages in the surrounding tissues in both groups and mast cells detected in EG-2 peri-implantation tissues. No giant multinucleated cells were detected in the surrounding tissues.

Thus, the pHEMA material in vivo did not cause a pronounced inflammatory reaction in the surrounding tissues under the conditions of this experiment, taking into account the cumulative assessment of the selected criteria.

DISCUSSION

In this work, the reparative processes of osteochondral tissues were investigated when the osteochondral defect was filled with an implant based on porous pHEMA. The choice of pHEMA was based on the literature data according to which this gel has good biocompatibility [10–13].

In vivo experiment detected single reticulofibrous bone trabeculae "sprouting" into the implant surface pores 30 days after implant introduction. This indicates the possibility of osseointegration of the material in a longer postoperative follow-up period. When pHEMA with chondrocytes was used, there was a slight increase

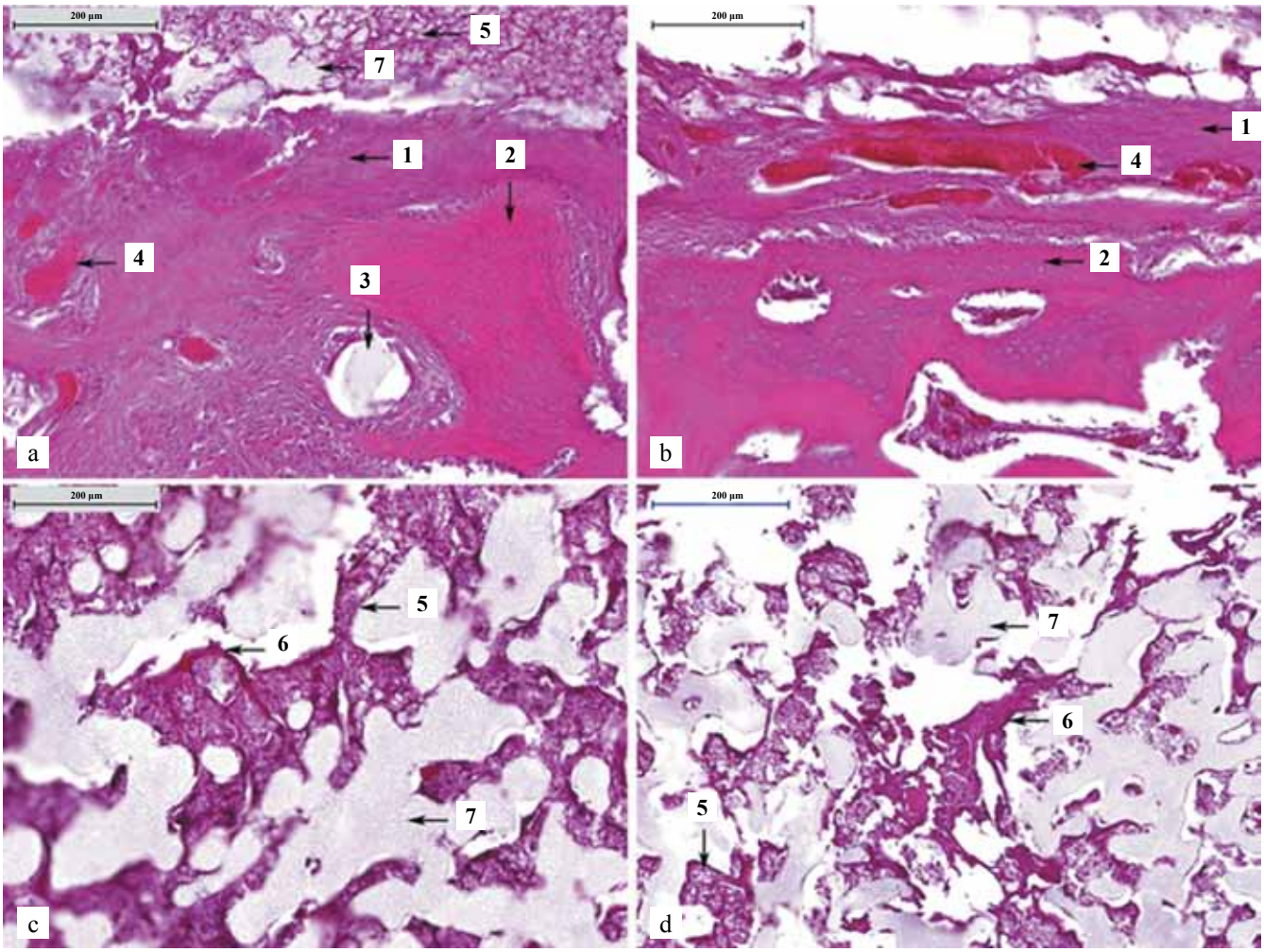

Fig. 6. Regenerates of osteochondral defects of the distal femoral epiphysis of rabbits, 30 days after implantation. H&E stain. Light microscopy, 200× magnification. a, c, experimental group 1; b, d, experimental group 2; a, b, implant cavity bed; c, d, implant. 1, connective tissue capsule in the implant cavity bed; 2, bone tissue inside the capsule; 3, pHEMA fragments inside the newly formed bone tissue; 4, vascular hyperemia; 5, connective tissue proper in the implant pores; 6, bone tissue in the implant pores; 7, pHEMA implant

in the area of chondrogenesis regions as compared to implants without cells.

At the same time, the totality of the results indicates poor integration of osteochondral tissues with the polymeric matrix of pHEMA. In terms of tissue response to the implant introduced, the polymeric matrix used should be referred to the category of biotolerant materials. The body response is characterized by formation of connective tissue capsule isolating the polymer matrix from the tissues and introduction of predominantly connective tissue into the implant pores. Thus, pHEMA implants showed minimal conductive properties with respect to osteochondral tissues when embedded into the osteoarticular defect.

The result obtained may be related to a number of physicochemical properties of the bioengineered matrix used [22]. It is known that the architecture of the pore space plays a key role in the delivery systems of cellular structures. Thus, maximum migration of chondrocytes [23] and osteoblasts [24] inside three-dimensional matrices is observed in the presence of 250–325 μm pores communicating with the surface. On the contrary, for fibroblasts, the highest level of adhesion and migration into the gel-based framework was observed at <100–160 μm pore sizes [25].

In the nomenclature of colloidal systems, pHEMA belongs to the category of macroporous polymers, i.e., it has a >1 μm pore size. In this study, pHEMA implants were used, which, according to optical microscopy, had irregularly shaped pores reaching a size of 300 μm × 120 μm. It should be noted that due to the presence of liquid phase in the gel, it is difficult to judge to what extent the studied implant cryosections (see Fig. 2, b, c) reflect the native structure of the material. At the same time, the obtained facts allow us to speak about the high degree of heterogeneity of pore size distribution in the samples. Indeed, the pores immediately near the implant surface were fundamentally smaller than the pores in the depth of the sample.

It can be hypothesized that the formation of a dense, finely porous pHEMA layer is associated with the features of polymer synthesis in polyethylene molds directly under the implant size (5 mm in diameter). However, the assumption that the mold walls have an influence over polymerization of the material in the boundary layer does not yet have a clear physicochemical substantiation.

Thus, the surface structure of hydrogels favored the migration of fibroblasts into pHEMA but did not promote cartilage or bone tissue migration. Consequently, it can be assumed that the implant sprouting of predominantly loose fibrous connective tissue in relation to insignificant volumes of osteochondral tissue is mainly caused by insufficient number of large pores on the surface of the used pHEMA implants.

It should be added that a possible reason for the extremely slow sprouting of osteochondral tissues into the implant may be the insufficient rigidity of the pHEMA platform used. Mechanical tests carried out on the material show that the elastic modulus of hydrogels was about an order of magnitude lower than those that ensure good chondrocyte proliferation on pHEMA [26]. At the same time, the established patterns of the dynamics of mechanical moduli with increasing strain rate (see Fig. 3, a), as well as the stress-strain relationship (see Fig. 3, b) were qualitatively consistent with the results of similar tests of canine intervertebral discs [27].

The aggregate data of histological examination 30 days after surgery implies that the level of tissue response to implantation of gels, including those with adhesive allogeneic chondrocytes, can be recognized as moderate against the background of the reaction caused by surgical trauma. The established facts do not contradict the data of other studies in which the absence of immune rejection of transplanted allogeneic chondrocytes in rabbits was noted, including, probably, due to their immunosuppressive activity [28].

In general, the information obtained in this work are consistent with the known facts about the influence of the physicochemical properties and surface structure of pHEMA on the biological activity of cells in in vitro experiments. This fact allows us to formulate the ways to optimize pHEMA synthesis to increase the biocompatibility of these hydrogels when used as implants for osteochondral defects in vivo.

CONCLUSION

This work is one of a limited number of in vivo studies that was aimed at investigating the possible implantation of pHEMA hydrogels to create engineering products with physical properties and structure close to native tissue. The hydrogels used in this work did not cause severe rejection response when implanted into rabbit femoral metaphysis, but sprouted predominantly fibrous connective tissue with an almost complete absence of osteochondral tissue in them.

The compatibility of the hydrogel with osteochondral tissue can be improved by creating a large-pore structure not only inside, but primarily at the surface of pHEMA. The results presented in the work suggest that reduction of heterogeneity in pore size distribution in the sample can be achieved by synthesizing pHEMA in a volume significantly larger than that required for implant fabrication. This will minimize the difference in pore size at the surface and inside the polymer.

In addition, attention is drawn to the literature data, where the increase in biocompatibility of hydrogel-based implants by means of modifying the polymer structure with solid fibers or particles is considered [29]. In particular, in a number of works [16, 17, 30], we showed

that inclusion of magnetic iron oxide nanoparticles into polyacrylamide gel composition leads to a significant increase in adhesion and cell proliferation on the surface of ferrogels in in vitro experiments. Thus, synthesis of pHEMA ferrogel samples with optimized pore sizes, as well as assessment of the tissue compatibility of these magnetic composites, is the direction of our future work.

The study was financially supported by State Assignment (No. 121032300335-1) of the Ministry of Health of the Russian Federation.

The authors declare no conflict of interest.

REFERENCES

1. *Jiang S, Guo W, Tian G, Luo X., Peng L, Liu S et al.* Clinical Application Status of Articular Cartilage Regeneration Techniques: Tissue-Engineered Cartilage Brings New Hope. *Stem Cells International*. 2020; ID 5690252, 16 pages. https://doi.org/10.1155/2020/5690252.
2. *Hangody L, Kish G, Kárpáti Z, Udvarhelyi I, Szigeti I, Bély M*. Mosaicplasty for the treatment of articular cartilage defects: application in clinical practice. *Orthopedics*. 1998; 21 (7): 751–756. PMID: 9672912.
3. *Benthien JP, Behrens P.* Autologous matrix-induced chondrogenesis (AMIC): a one-step procedure for retropatellar articular resurfacing. *Acta Orthop Belg*. 2010; 76 (2): 260–263. PMID: 20503954.
4. *Davies RL, Kuiper NJ.* Regenerative Medicine: A Review of the Evolution of Autologous Chondrocyte Implantation (ACI) Therapy. *Bioengineering (Basel)*. 2019; 6 (1): 22. doi: 10.3390/bioengineering6010022.
5. *Behrens P, Bitter T, Kurz B, Russlies M*. Matrix associated autologous chondrocyte transplantation: a 5 year follow up. *Knee.* 2006; 13 (3): 194–202. doi: 10.1016/j.knee.2006.02.012.
6. *Park YB, Ha CW, Rhim JH, Lee HJ.* Stem Cell Therapy for Articular Cartilage Repair: Review of the Entity of Cell Populations Used and the Result of the Clinical Application of Each Entity. *The American journal of sports medicine*. 2018; 46 (10): 2540–2552. https://doi.org/10.1177/0363546517729152.
7. *Gerasimov SA, Tenilin NA, Korytkin AA, Zykin AA.* Surgical treatment of localized injuries to articular surface: the current state of the issue. *Polytrauma*. 2016; 1: 63–69.
8. *Dobreikina A, Shklyar T, Safronov A, Blyakhman F*. Biomimetic gels with chemical and physical interpenetrating networks. *Polym Int.* 2018; 67: 1330–1334. doi 10.1002/pi.5608.
9. *Tejo-Otero A, Fenollosa-Artés F, Achaerandio I, Rey-Vinolas S, Buj-Corral I, Mateos-Timoneda MÁ et al.* Soft-Tissue-Mimicking Using Hydrogels for the Development of Phantoms. *Gels*. 2022; *8*: 40. https://doi.org/10.3390/gels8010040/.
10. *Mokry J, Karbanova J, Lukas J, Paleckova V, Dvorankova B.* Biocompatibility of HEMA copolymers designed for treatment of CNS diseases with polymer-encapsulated cells. *Biotechnol Prog*. 2020; 16: 897–904.
11. *Rotaru I, Olaru.* Mechanical behaviour of p(HEMA) hydrogel for disc prosthesis on lumbar spine. *Optoelectronics and Advanced Materials*. 2014; 16 (7–8): 881–886.
12. *Kubinová Š, Horák D, Hejcl A, Plichta Z, Kotek J, Proks V et al.* SIKVAV-modified highly superporous PHEMA scaffolds with oriented pores for spinal cord injury repair. *J Tissue Eng Regen Med*. 2015; 9: 1298–1309.
13. *Cao J, Liu Z, Zhang L, Li J, Wang H, Li X.* Advance of Electroconductive Hydrogels for Biomedical Applications in Orthopedics. *Advances in Materials Science & Engineering*. 2021; 1–13. doi: 10.1155/2021/6668209.
14. *Hoffman AS.* Hydrogels for biomedical applications. *Adv Drug Deliver Rev*. 2012; 64: 18–23. https://doi.org/10.1016/j.addr.2012.09.010.
15. *Kukolevska JS, Gerashchenko II, Borysenko MV, Pakhlov EM, Machovsky M, YushchenkoTI.* Synthesis and Examination of Nanocomposites Based on Poly(2-hydroxyethyl methacrylate) for Medicinal Use. *Nanoscale Research Letters*. 2017; 12: 133. doi 10.1186/s11671-017-1881-7.
16. *Blyakhman FA, Safronov AP, Makeyev OG, Melekhhin VV, Shklyar TF, Zubarev AYu et al.* Effect of the polyacrylamide ferrogel elasticity on the cell adhesiveness to magnetic composite. *J Mechanics in Medicine and Biology*, 2018; 18 (6): 1850060 (13 pages) https://doi.org/10.1142/S0219519418500604.
17. *Blyakhman FA, Makarova EB, Fadeyev FA, Lugovets DV, Safronov AP, Shabadrov PA et al.* The Contribution of Magnetic Nanoparticles to Ferrogel Biophysical Properties. *Nanomaterials*. 2019; 9: 232. doi: 10.3390/nano9020232.
18. *Karpushkin E, Dušková-Smrčková M, Šlouf M, Dusek K*. Rheology and porosity control of poly(2-hydroxyethyl methacrylate) hydrogels. *Polymer* 2013; 54: 661–672. http://dx.doi.org/10.1016/j.polymer.2012.11.055.
19. *Stupina TA, Petrovskaia NV, Stepanov MA.* Study regeneration of cartilage and bone tissue in modeling slit-shaped osteochondral defects patellar femoral condyle surface in experiment. *International Journal of applied and fundamental research*. 2015; 5-1: 68–71. URL: https://applied-research.ru/ru/article/view?id=6764.
20. GOST RISO 10993.6-2011 Izdeliya meditsinskie. Otsenka biologicheskogo deystviya meditsinskikh izdeliy. Chast' 6. Issledovaniya mestnogo deystviya posle implantatsii.
21. *Fung YC, Cowin SC.* Biomechanics. Mechanical Properties of Living Tissues. *Journal of Biomechanical Engineering*. 1994; 61 (4): 1007. doi: 10.1115/1.2901550.
22. *Chen L, Yan C, Zheng Z.* Functional polymer surfaces for controlling cell behaviors. *Materials Today*. 2018; 21 (1): 38–59. https://doi.org/10.1016/j.mattod.2017.07.002.
23. *Lien SM, Ko LY, Huang TJ.* Effect of pore size on ECM secretion and cell growth in gelatin scaffold for articular cartilage tissue engineering. *Acta Biomater*. 2009; 5 (2): 670–679. doi: 10.1016/j.actbio.2008.09.020.

24. *Murphy CM, Haugh MG, O'Brien FJ.* The effect of mean pore size on cell attachment, proliferation and migration in collagen-glycosaminoglycan scaffolds for bone tissue engineering. *Biomaterials.* 2010; 31 (3): 461–466. doi: 10.1016/j.biomaterials.2009.09.063.
25. *Harley BA, Kim HD, Zaman MH, Yannas IV, Lauffenburger DA, Gibson LJ.* Microarchitecture of three-dimensional scaffolds influences cell migration behavior via junction interactions. *Biophys J.* 2008; 95 (8): 4013–4024. doi: 10.1529/biophysj.107.122598.
26. *Passos MF, Carvalho NMS, Rodrigues AA, Bavaresco VP, Jardini AL, Maciel MRW et al.* PHEMA hydrogels obtained by infrared radiation for cartilage tissue engineering. *International journal of chemical engineering*. 2019; ID 4249581. https://doi.org/10.1155/2019/4249581.
27. *Gloria A, Causa F, De Santis R, Netti PA, Ambrosio L.* Dynamic-mechanical properties of a novel composite intervertebral disc prosthesis. *J Mater Sci: Mater Med*. 2007; 18: 2159–2165 doi 10.1007/s10856-007-3003-z.
28. *Moskalewski S, Hyc A, Osiecka-Iwan A.* Immune response by host after allogeneic chondrocyte transplant to the cartilage. *Microsc Res Tech*. 2002; 58 (1): 3–13. doi: 10.1002/jemt.10110.
29. *Aleksandrov VN, Sokolova MO, Komarov AV, Mikhailova EV, Kokorina AA, Kriventsov AV.* Cell technologies in cartilage regeneration. *Tsitologiya.* 2020; 62 (3): 160–172. doi: 10.31857/S0041377120030025.
30. *Kurlyandskaya GV, Blyakhman FA, Makarova EB, Buznikov NA, Safronov AP, Fadeyev FA et al.* Functional magnetic ferrogels: From biosensors to regenerative medicine. *AIP Advances*. 2020; 10: 125128. https://doi.org/10.1063/9.0000021.

The article was submitted to the journal on 25.04.2022